ACS APPLIED MATERIALS & INTERFACES

Research Article

www.acsami.org

Complementary Effects of Nanosilver and Superhydrophobic Coatings on the Prevention of Marine Bacterial Adhesion

Tao Liu,*[,†] Bing Yin,[†] Tian He,[‡] Na Guo,[†] Lihua Dong,[†] and Yansheng Yin*[,†]

[†]Institute of Marine Materials Science and Engineering, Shanghai Maritime University, Shanghai 200135, China

[‡]College of Material, Chemistry and Chemical Engineering, Hangzhou Normal University, Hangzhou 310036, China

ABSTRACT: A superhydrophobic coating composed of silver nanoparticles enclosed in multilayered polyelectrolyte films was deposited onto copper with the aim of preventing bacterial adhesion. Observations from scanning electron microscopy (SEM) and atomic force microscopy (AFM) showed that the amplified exponential growth of the multilayers could induce distinguishable, hierarchical micro- and nanostructures simultaneously. This growth caused the surface roughness to amplify in a lotus-leaf-like manner. UV/visible spectroscopy, X-ray photoelectron spectroscopy (XPS), and transmission electron microscopy (TEM) confirmed the formation of well-dispersed Ag^0 nanoparticles (with sizes from 4−6 nm) in the films. SEM and fluorescence microscope images of the exposed surfaces revealed that the pattern of adhesion and the density of bacterial cells differed depending on the surface energy and the number of Ag^+ ions released during the various immersion time periods. The complementary effects of nanosilver and superhydrophobic coatings can help to effectively reduce bacterial adhesion and the formation of biofilms.

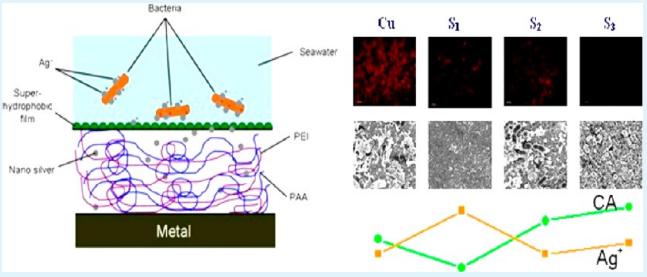

KEYWORDS: *microbial biofilm, bacterial adhesion, nanosilver, superhydrophobic*

1. INTRODUCTION

Biofouling is a costly and serious problem facing the marine industry. Many issues such as pressure losses in pipe systems, increased drag on ship hulls, down time for cleaning, and replacing mechanical parts are caused by biofouling.[1] Generally, fouling is a phenomenon in which marine microorganisms bind to surfaces to form a conditioning layer. This layer then provides an easily accessible platform for other aquatic species, such as algae and invertebrate, to attach and proliferate.[2,3]

To combat surface fouling, two different approaches have been proven to be effective. The first approach is the nature-inspired coatings with superhydrophobic properties that have been designed for underwater applications.[4,5] Superhydrophobic surfaces can be fabricated from materials with a combination of low surface energy and high surface roughness. Several types of superhydrophobic films are based on this concept, including those fabricated with silica nanoparticles,[6] carbon nanotubes,[7] and polymers.[8] The antibiofouling properties of superhydrophobic coatings have been investigated.[9] Compared to normal substrates which exhibit fouling within a day, almost no microorganisms attach to the superhydrophobic surfaces in the first weeks of immersion. However, after long exposure to real marine environment, the antifouling property of the superhydrophobic coatings will become gradually deteriorated. In the second approach, TiO_2, Cu_2O, and Ag nanoparticles have been widely used for their bactericidal activities.[10] Silver nanoparticles have been shown to be especially bactericidal.[11,12] Antimicrobial silver ions or nanoparticles have been grown on or embedded in polyamides,[13] polyelectrolyte multilayers,[14,15] fiber glass,[16] other polymers[17] and in hydrogels[18] to form antimicrobial films. However, poor metal-to-material adhesion and the incomplete control of the nanoparticles released in the liquid medium are the main drawbacks of the method. In addition, Ag nanoparticles will only be effective as antibacterial agents for a short period of time until the Ag^+ is exhausted. This is particularly important for systems in flowing liquids.

To address the limitations of the current coating procedures, some methods were created to be successful. Rubner and co-workers constructed thin film coatings with two distinct layered regions: a reservoir for the loading and releasing of bactericidal chemicals and a nanoparticle surface cap with immobilized bactericides;[19] Sambhy and co-workers reported another type of dual-action antibacterial material based on silver bromide nanoparticles and a cationic polymer;[20] Petronis et al. designed and prepared silicone surfaces with microstructures and well-defi ned surface chemistry for antifouling purposes.[21] This paper reports the synthesis of superhydrophobic films that contain silver nanoparticles. This method requires forming a polyelectrolyte-metal ion complex, adsorbing layers of the complex and layers of a polyanion, and reducing the silver ions.[22,23] This method has several advantages. First, nanoparticles are dispersed throughout the film because the silver ions are well distributed along the polymer chains. The surrounding polymer limits particle aggregation, yielding small particles and ensuring the

Received: June 11, 2012
Accepted: August 31, 2012
Published: August 31, 2012

controlled release of these particles. Second, the nanosilvers are used as microbial agents. Once the superhydrophobic coatings become deteriorated, nanosilvers can release to be used for preventing microbial adhesion and for killing bacteria.

2. EXPERIMENTAL METHODS

2.1. Surface Coating Preparation. The multilayer films were constructed according to the method referred in the reference of Ji.[24] Fresh copper substrates were alternately deposited in aqueous solutions of a polycation (1 mg/mL polyethyleneimine (PEI, M.W. 70 000), pH 7.0, with 2 mM silver nitrate) and a polyanion (3 mg/mL poly(acrylic acid) (PAA, M.W. 450 000), pH. 5.0) for 15 min followed by washing with pure water three times and drying with N_2 respectively. The immersion steps were repeated until 16 layers (8 bilayers) of films were adsorbed. Different from the method reported by Prof. Ji, after the layers were adsorbed, the polyelectrolyte multilayers films (PEMs) were immersed into 1 mM $NaBH_4$ to reduce the Ag^+ ions to silver nanoparticles and dried with N_2 (S_1). Then a layer of (tridecafluoroctyl)-triethoxysilane (Fluoro-silane) was deposited on the substrate by chemical vapor deposition to obtain a surface with low surface energy (S_3). In addition, in order to assess the influence of nanosilvers on biofilm development, a coating using S_3 method except adding silver ions (S_2) was also prepared. So three types of coatings were prepared in this experiment for comparison.

S_1: PEMs + Ag^0

S_2: PEMs + Fluoro-silane

S_3: PEMs + Ag^0 + Fluoro-silane

2.2. Coatings Analysis. A scanning electron microscope (SEM, JEOL JSM-7500F) and an atomic force microscope (AFM, SII Nanonavi E-Sweep) were used to analyze the surface morphology of the film, and a high-resolution transmission electron microscope (HRTEM, JEM 2100F) was used to observe the size and distribution of the silver nanoparticles. To be observed by TEM, we deposited only 8 multilayers on a grid with carbon film for TEM imaging. The reduction of the silver nanoparticles was monitored by examining the UV/visible spectra on a PerkinElmer Lambda 35 spectrophotometer. The contact angles were measured by a JC2000A CA system at ambient temperature.

A scanning electron microscope (SEM, JEOL JSM-7500F) was used to measure the thickness of the multilayer films. In case of thickness determination, the PEI/PAA multilayer films were constructed onto the silicon wafer via the same layer-by-layer deposition as described above. After the deposition of the desired number of polyelectrolyte layers, the silicon wafers were snapped and the cross section of the multilayer films was imaged by SEM. The thickness of the multilayers was calculated from the mean of three separate experiments.

Before chemical vapor deposition, the molecular physicochemical properties of the nanocomposite films were assessed using X-ray photoelectron spectroscopy (XPS, AXIS Ultra with monochromatic Al Ka radiation at 1486.6 eV). The following core levels were analyzed: N 1s, C 1s, O 1s, and Ag 3d.

The Ag^+ ion release kinetics of the S_1 and S_3 coating into deionized water were regularly monitored by ICP-MS (inductively coupled plasma-mass spectroscopy) until 13 days of exposure.

2.3. Inoculum Preparation. The strain of Sulfate-reducing bacteria (*D.salexigens*, Guangdong Microbial Sci. and Tech. Institute) were used as test microorganisms in the antibiofouling experiments. This type of bacteria was selected because SRB was often reported to promote or accelerate membrane biofouling and biocorrosion.[25] SRB was cultured in a BioMero Bact API 20 solution (N_2 environment, 37 ± 1 °C).

2.4. Antibiofouling Tests. The antibiofouling tests focused on the performance of S_1, S_2 and S_3 in preventing bacterial adhesion and reproduction on the surfaces. The samples were immersed in the liquid medium of SRB at the stationary growth phase.

The surfaces (Φ = 1.2 cm) in the antibiofouling tests were observed with a scanning electron microscope according to the method described by Zhu.[26] After the samples were immersed vertically in the liquid medium of SRB at 37 ± 1 °C for 1 day and 7 days, respectively, they were washed with PBS. The bacteria on the surfaces were then fixed in a 3% (v/v) glutaraldehyde solution for 5 h at 4 °C. After the fixation, the surfaces were rinsed with PBS to remove any remaining glutaraldehyde. Step dehydrations were subsequently performed on each of the samples with 25, 50, 75, and 100% ethanol for 10 min to reduce their water content. Finally, the samples were air-dried, and the surfaces were prepared for observation in SEM. The number of attached bacteria was determined using an fluorescence microscope (NIKON/Ti-E).

3. RESULTS AND DISCUSSION

Herein, the amplified exponential growth of a multilayer of polyelectrolytes as a facile method to construct hierarchical

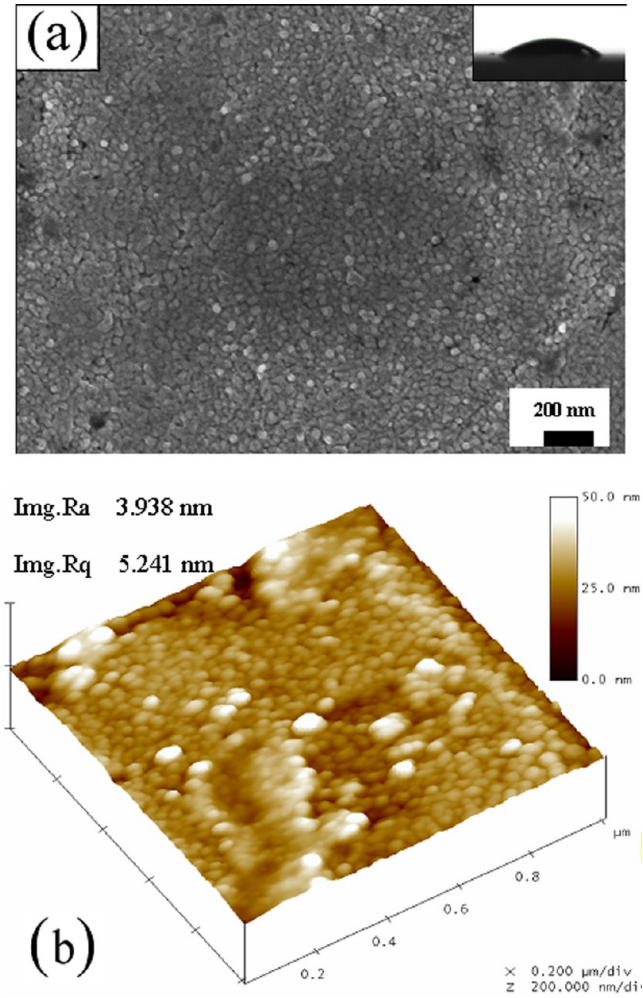

Figure 1. (a) SEM and (b) AFM images of S_1 (16 multilayer films embedded with nanosilver).

nanostructures was studied. S_1 (shown in Figure 1) has a rough surface (the mean roughness R_a is approximately 3.9 nm) with a globe-shaped topography on the order of ~50 nm and the contact angle of the surface is about 35°, which can be further transformed into superhydrophobic surface. The chemical vapor deposition of (tridecafluoroctyl)-triethoxysilane onto the above surface mimics the bioinspired combination of low surface energy species and hierarchical topographic features. S_3 (shown in Figure 3) has vermiculate patterns on the order of 300 nm and nanoconvexities on the order of 50 nm. The superhydrophobicities of the film are believed to be due to the presence of cooperative, binary structures at nanometre level that reduce the energies of the surfaces. The silver ions can enhance the excessive diffusion and the exponential growth of the polyethyleneimine

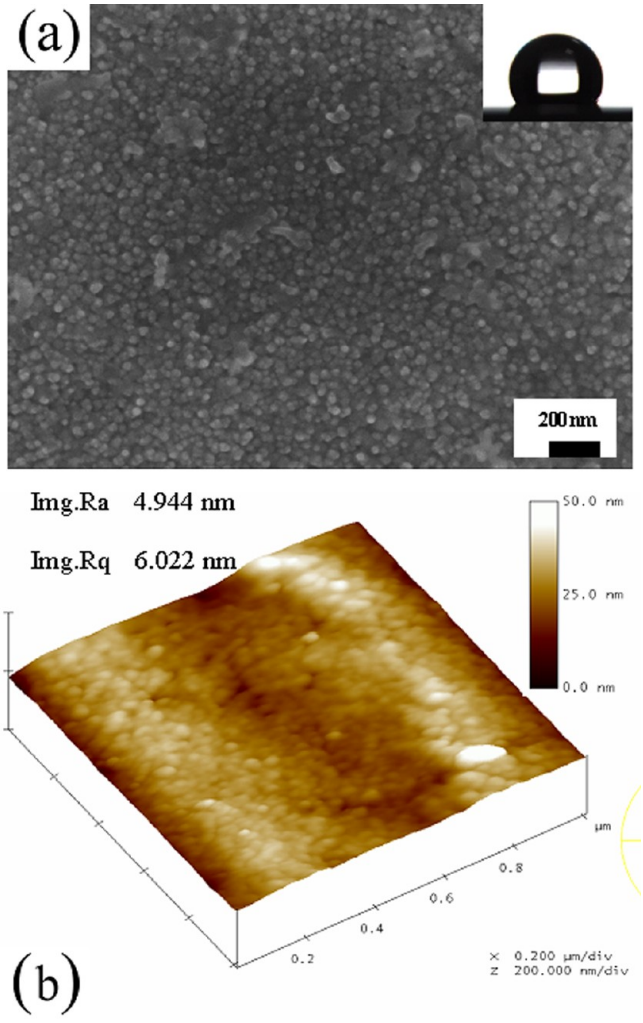

Figure 2. (a) SEM and (b) AFM images of S_2 (hydrophobic coating without silver ions).

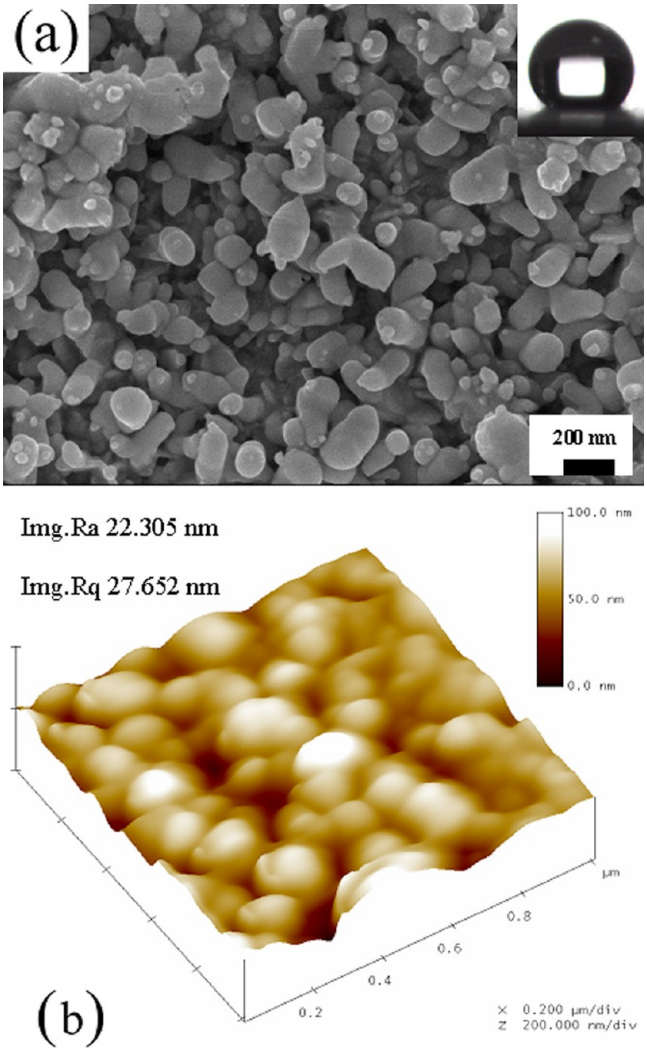

Figure 3. (a) SEM and (b) AFM images of S_3 (superhydrophobic coating with nanosilvers).

(PEI)/poly(acrylic acid) (PAA) multilayers, which help the construction of the hierarchical micro- and nanostructures necessary to form the superhydrophobic surface. To evaluate the effect of silver ions on the formation of superhydrophobic surface, a coating (S_2) without the use of silver ions was prepared (shown in Figure 2). The hydrophobicities of the S_2 and S_3 were investigated by probing the contact angles (CA) via the sessile-drop and tilting-plate measuring methods. The S_2 (with structure as shown in Figure 2) exhibits a contact angle as high as 126°, but the tilt angle is more than 37°. In sharp contrast, the S_3 (with structure as shown in Figure 3) has a contact angle as high as 152°and the tilt angle as low as 8°. Differences of surface roughness and contact angles indicate silver ions play an important role in the surface morphology constructing. The silver ion, the metal ligand that can form a complex with PEI and PAA, was used to enhance the exponential growth of the PEI/PAA multilayers and also to increase the surface roughness (shown in Figure 4).

In addition, silver is more toxic element to microorganisms than many other metals in the following sequence: Ag > Hg > Cu > Cd > Cr > Pb > Co > Au > Zn > Fe > Mn > Mo > Sn.[27] And nanosilver exert more efficient than silver ions and other silver salts in mediating their antimicrobial activity.[28] So the PEI-metal ion complex/PAA films were deposited on a surface and

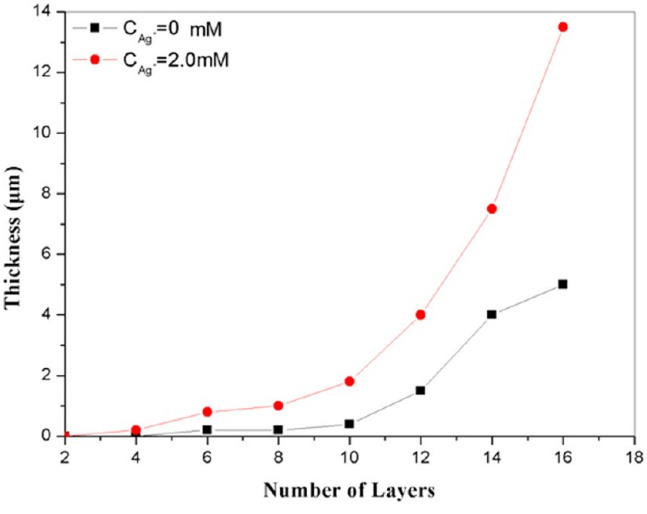

Figure 4. Variation in the thickness of PAA/PEI (square) and PAA/PEI $+Ag^+$ (circle) multilayered films vs number of dipping cycles. The thickness was determined by the scanning electron microscopy (SEM) investigation of the cross-section of the multilayer. Results represent the mean of three separate experiments.

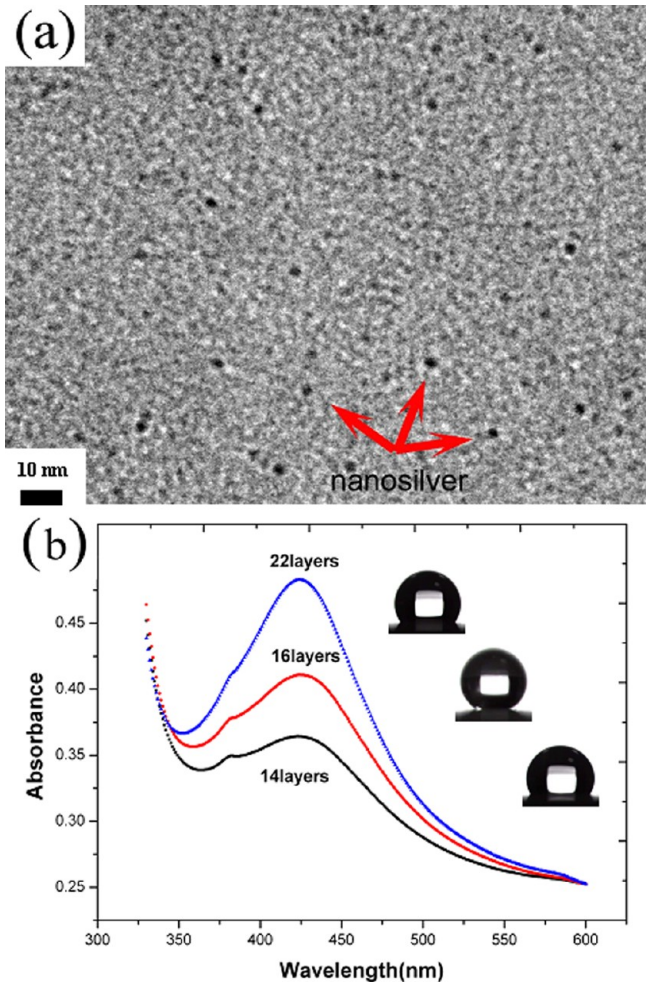

Figure 5. (a) TEM image and (b) UV−visible spectra of multilayer films embedded with nanosilver without fluorosilane.

subsequently reducing the metal ions with $NaBH_4$ to form nanoparticles as following eq 1. This affords a convenient method for controlling the amount of metal ions in the film, which in turn allows controlling particle size after reduction.

$$NaBH_4 + AgNO_3 + 3H_2O \rightarrow Ag + NaNO_3 + B(OH)_3 + 3.5H_2 \quad (1)$$

The TEM image in Figure 5a shows that the particles produced by $NaBH_4$ reduction are relatively monodisperse (with diameters of 3.0−4.0 nm). The surface plasmon absorbance resulting from the Ag^0 particles increased with the number of layers in the film, as expected (Figure 5b). However, the contact angle increased from 123 to 152°as the layers of film increased to 16 layers and then decreased to 125° after 16 layers, indicating that the morphology at 16 layers is the most suitable for constructing superhydrophobic surfaces.

The nanosilver films were mainly composed of C, O, N and Ag, and the atomic concentrations of silver in the films was 3.13%, as revealed by XPS analyses. The high-resolution Ag 3d spectra recorded for the film is shown in Figure 6. The Ag 3d spectrum shows a signal at 367.6 eV that corresponds to metallic silver. Moreover, the modified Auger parameter was calculated by adding the peak binding energy of the most intense photoemission peak (Ag 3d5/2) to the kinetic energy of the sharpest Auger emission (M4N45N45 Auger peak). The Auger

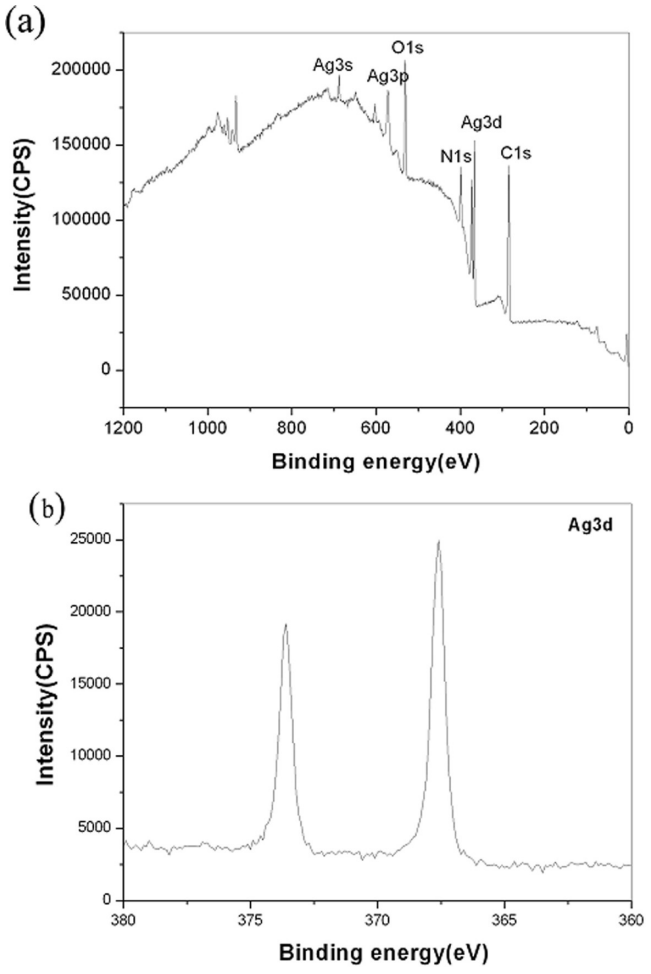

Figure 6. (a) XPS survey spectrum and (b) high-resolution XPS spectra of Ag 3d of S_1 (16 multilayer films embedded with nanosilver).

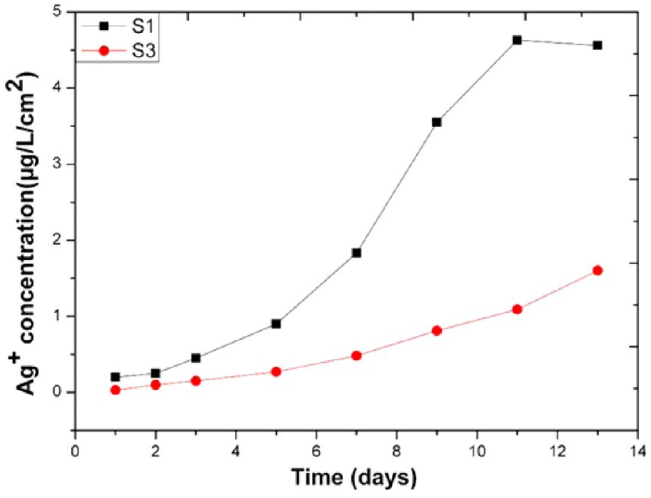

Figure 7. Silver ion release kinetics in deionized water for the S_1 and S_3.

parameter for silver was determined to be 725.8 eV, which confirms that silver was predominantly in the metallic form.[29]

Antibiofouling tests show that the bacterial density, the degree of aggregation and biofilm coverage are closely related with surface hydrophobicities or silver ions release in different adherent stages. In the first day immersion, few SRB bodies could be found on the S_2 surface and S_3; however, dense layers of

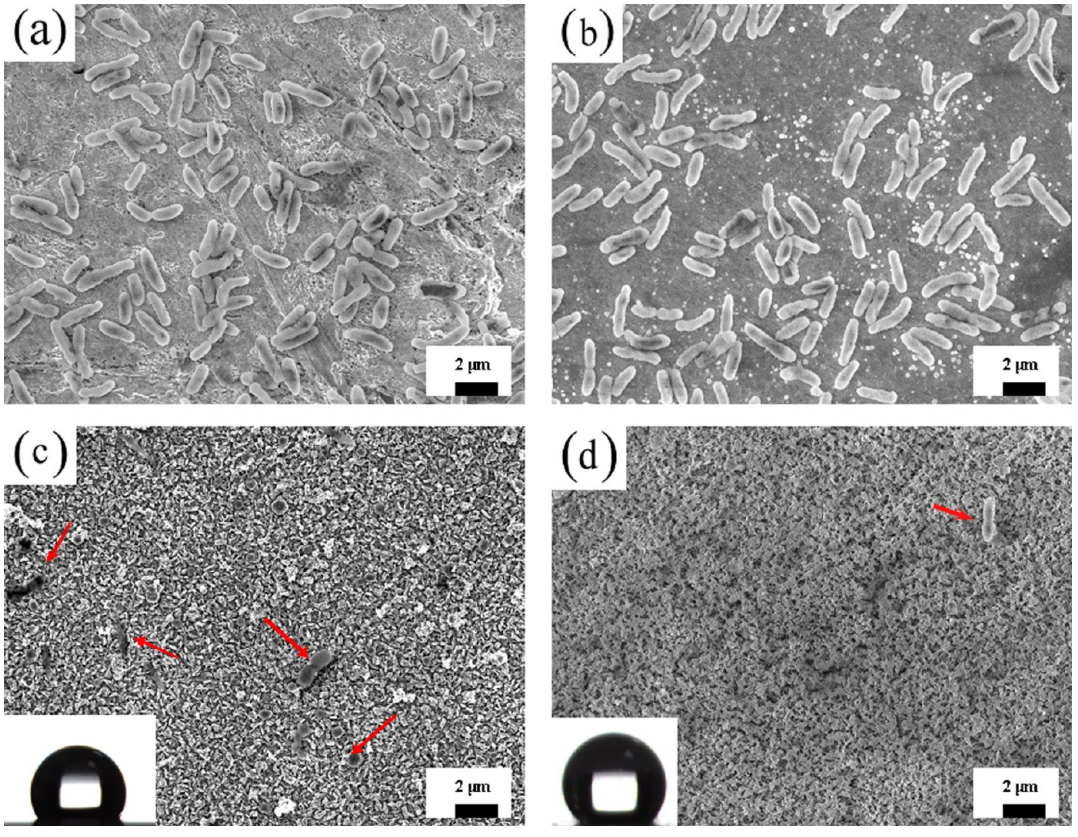

Figure 8. SEM images of SRB adhered to the (a) copper, (b) S_1, (c) S_2, (d) S_3 after immersion in suspension of SRB for 1 day (red arrow signs SRB).

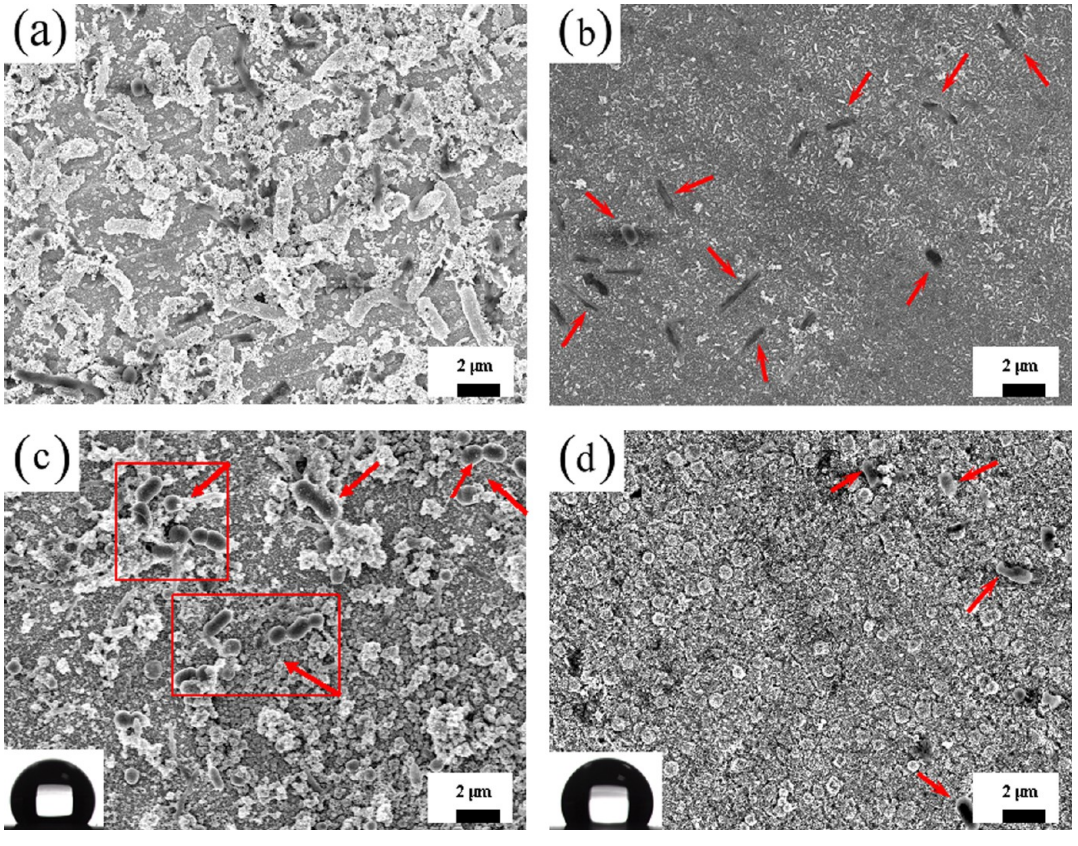

Figure 9. SEM images of SRB adhered to the (a) copper, (b)S_1, (c) S_2, (d) S_3 after immersion in suspension of SRB for 7 days (red arrow signs SRB).

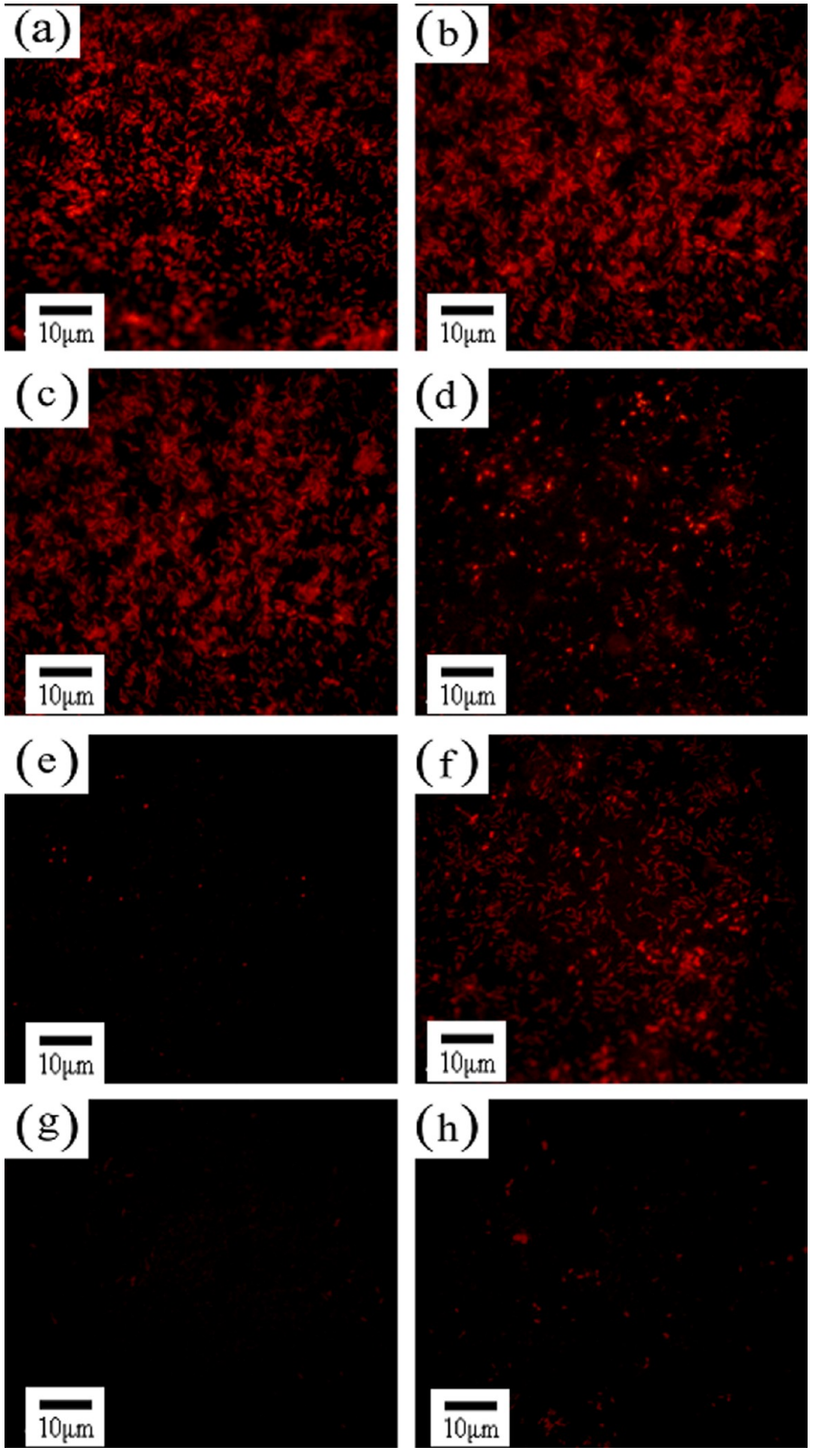

Figure 10. Fluorescence microscope images of attached bacteria on the copper (a) 1 day, (b) 7 days; S_1 (c) 1 day, (d) 7 days; S_2 (e) 1 day, (f) 7 days; S_3 (g) 1 day, (h) 7 days.

bacteria covered the copper surface and S_1, which have no hydrophobic surfaces (Figure 8). In the area of marine fouling, hydrophobicity has been shown to deter colonisation of invertebrate shells[30,31] and to alter settlement of algae,[32] barnacles,[33] and bacteria.[34] The change in wettability of a surface that results from surface roughness, i.e. topography, is likely to be a contributing factor to these responses. On the other hand, because biofouling originates from biological entities suspended

dx.doi.org/10.1021/am301049v | *ACS Appl. Mater. Interfaces* 2012, 4, 4683−4690

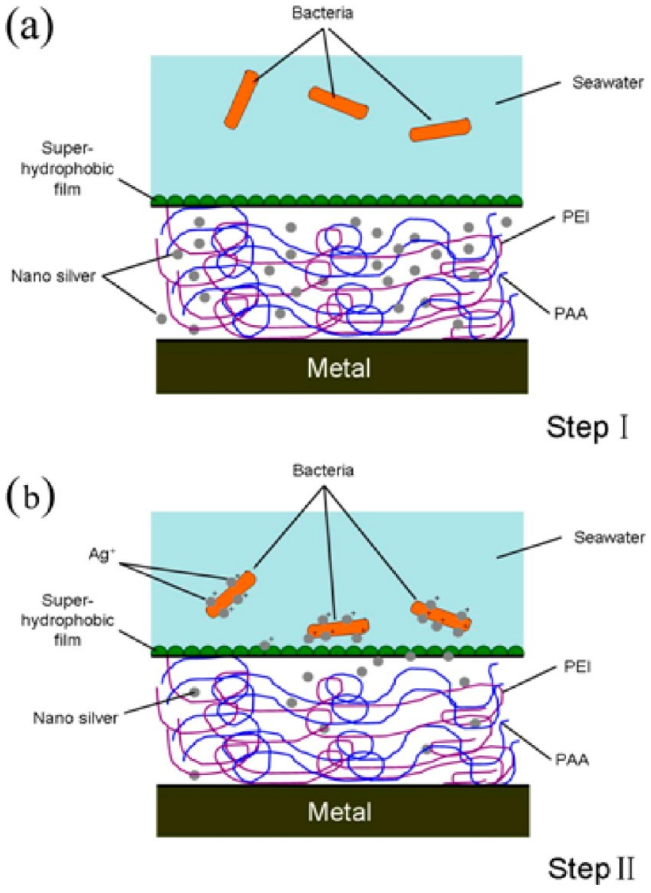

Figure 11. Schematic representations of preventing microbial adhesion and killing bacteria steps in seawater.

in water, minimization of water contact with the solid surface may also be an effective tool in preventing biofouling. This, in principle, may be achieved by keeping an air film between the solid and the water, an approach that involves wetting phenomena in a solid−water−air system.

When the samples were immersed in the SRB medium for 7 days, SEM and fluorescence microscope images (Figure 10) showed a higher density of aggregated cells covered on the copper surface and S_2 while few SRB cells adhered to S_1 and S_3 (Figure 9). It was interested to find that more bacteria attached to the surfaces with increasing of immersion time except coating S_1. The possible results could be foud out from the ion release kinetics (Figure 7), the release rate of Ag^+ was ~2 $\mu g/L/cm^2$ at day 7 for S_1, it is highly likely that this concentration of Ag^+ ions would have an antimicrobial effect on reducing the number of SRB attached to the surface. By compared with S_1 (Ag^+ ions concentration 2 $\mu g/L/cm^2$) and S_2 (the contact angle 120°), S_3 still has the most excellent performance on prevention of bacterial adhesion at 7 days though the contact angle decreased from 152 to 123° and Ag^+ ion concentration was only ~0.5 $\mu g/L/cm^2$. It suggested that attachment and proliferation of bacterial cells were indeed influenced by complementary effects of nanosilver and hydrophobic coatings .

The mechanism of preventing microbial adhesion is shown in Figure 11. According to previous studies,[35] silver antimicrobial activity is related to Ag^+ ion progressive release from the embedded nanoparticles into the surrounding aqueousmedium. In the beginning of the immersion, silver ions embedded in the films of S_1 and S_3 release slowly, the concentration of Ag^+ ions can not take antimicrobial effect. Bacterial adhesion is closely associated with the wetting phenomena of surface in the solid−water−biological matter system. The low surface energy and rough surface topography may prevent adhesion.[36] So the amount of SRB adhered onto the surfaces was in the following sequence: $S_1 > S_2 > S_3$, which is inversely proportional to the contact angles sequence: $S_1 < S_2 < S_3$. As the immersion time increases, silver nanoparticles generate a sustained flux of Ag^+ ions. Then, Ag^+ ions bind to thiol groups in biological enzymes and disrupt the bacterial respiratory chain, generating reactive oxygen species (ROS) that can lead to oxidative stress and cell damage.[37] The amount of SRB attached to the surfaces was in another sequence: $S_2 > S_1 > S_3$. The S_1 coating shows the better antifouling properties than S_2 after 7 days, which can be attributed to the Ag^+ ions release. In addtion, the fluoro-silane coatings could control the release of Ag^+ ion effectively observed for curve trend of S_1 and S_3, it is very valuable for long-term use in prevention bacterial adhesion.

4. CONCLUSIONS

In conclusion, a facile method for developing superhydrophobic surfaces from a fluorinated multilayer that also contain silver nanoparticles has been demonstrated. In the preparation process, the silver ions enhanced the exponential growth of PEI/PAA multilayers, and the construction of the hierarchical micro- and nanostructures necessary for the formation of superhydrophobic surfaces. During initial immersion, the superhydrophobic coating can efficiently prevent the adhesion of SRB. By this approach, the probability of the suspended biological entities adhering to the solid surface could be greatly reduced. After 7 days of immersion, the superhydrophobicity of the coating decreased. However, the silver nanoparticles began to generate a sustained flux of Ag^+ ions, which damaged the bacterial cells and reduced the bacterial adhesion. This work shows that controlling the chemistry and topology of surfaces are important when designing marine coatings that can efficiently prevent or reduce bacterial adhesion.

AUTHOR INFORMATION

Corresponding Author

*E-mail: liutao@shmtu.edu.cn (T.L.); yinys@shmtu.edu.cn (Y.Y.).

Notes

The authors declare no competing financial interest.

ACKNOWLEDGMENTS

This research was supported by The National Natural Science Foundation (51003056), Shanghai Education Commission Research and Innovation key program (12YZ121) and Innovation Program of Shanghai Municipal Science and Technology (10170502400).

REFERENCES

(1) Jones, W. L.; Sutton, M. P.; McKittrick, L. *Biofouling* **2011**, *27*, 207−215.

(2) Olsen, S. M.; Pedersen, L. T; Laursen, M. H.; Kiil, S.; Johansen, K. D. *Biofouling* **2007**, *23*, 369−383.

(3) Kristensen, J. B.; Meyer, R. L.; Laursen, B. S.; Shipovskov, S.; Besenbacher, F.; Poulsen, C. H. *Biotechnol. Adv.* **2008**, *26*, 471−481.

(4) Carman, M. L.; Estes, T. G.; Feinberg, A. W.; Schumacher, J. F.; Wilkerson, W.; Wilson, L. H.; Callow, M. E.; Callow, J. A.; Brennan, A. B. *Biofouling* **2006**, *22*, 11−16.

(5) Schumacher, J. F.; Carman, M. L.; Estes, T. G.; Feinberg, A. W.; Wilson, L. H.; Callow, M. E.; Yang, J. J.; Zhang, Z. Z.; Men, X. H.; Xu, X. H. *Appl. Surf. Sci.* **2009**, *255*, 9244−9247.
(6) Ling, X. Y.; Phang, I. Y.; Vancso, G. J.; Huskens, J.; Reinhoudt, D. N. *Langmuir* **2009**, *25*, 3260−3263.
(7) Yang, J.; Zhang, Z. Z.; Men, X. H.; Xu, X. H. *Appl. Surf. Sci.* **2009**, *255*, 9244−9247.
(8) Wu, D.; Ming, W.; Benthem, R. V.; With, G. D. *J. Adhes. Sci. Technol.* **2008**, *22*, 1869−1881.
(9) Zhang, H.; Lamba, R.; Lewis, J. *Sci. Technol. Adv. Mat.* **2005**, *6*, 236−240.
(10) Silver, S.; Phung, L. T.; Silver, G. *J. Ind. Microbiol. Biot.* **2006**, *33*, 627−634.
(11) Rai, M.; Yadav, A.; Gade, A. *Biotechnol. Adv.* **2009**, *27*, 76−83.
(12) Morones, J. R.; Elechiguerra, J. L.; Camacho, A.; Holt, K.; Kouri, J. B.; Ramirez, J. T.; Yacaman, M. J. *Nanotechnology* **2005**, *16*, 2346−2353.
(13) Damm, C.; Munstedt, H. *Appl. Phys. A-Mater.* **2008**, *91*, 479−486.
(14) Dai, J. H.; Bruening, M. L. *Nano Lett.* **2002**, *2*, 497−501.
(15) Lee, D.; Cohen, R. E.; Rubner, M. F. *Langmuir* **2005**, *21*, 9651−9659.
(16) Nangmenyi, G.; Yue, Z. R.; Mehrabi, S.; Mintz, E.; Economy, J. *Nanotechnology* **2009**, *20*, 18−21.
(17) Sambhy, V.; MacBride, M. M.; Peterson, B. R.; Sen, A. *J. Am. Chem. Soc.* **2006**, *128*, 9798−9808.
(18) Uygun, M.; Kahveci, M. U.; Odaci, D.; Timur, S.; Yagci, Y. *Macromol. Chem. Physic.* **2009**, *210*, 1867−1875.
(19) Li, Z.; Lee, D.; Sheng, X.; Cohen, R. E.; Ruber, M. F. *Langmuir* **2006**, *22*, 9820−9823.
(20) Sambhy, V.; MacBride, M. M.; Peterson, B. R.; Sen, A. *J. Am. Chem. Soc.* **2006**, *128*, 9798−9881.
(21) Petronis, S.; Berntsson, K.; Gold, J.; Gatenholm, P. *J. Biomater. Sci., Polym. Ed.* **2000**, *11*, 1051−1053.
(22) Francolini, I.; Crisante, F.; Martinelli, A. *Acta. Biomater.* **2012**, *8*, 549−558.
(23) Fu, J. H.; Ji, J.; Feng, D. Z.; Shen, J. C. *J. Biomed. Mater. Res.* **2006**, *79*, 665−674.
(24) Ji, J.; Fu, J. H.; Shen, J. C. *Adv. Mater.* **2006**, *18*, 1441−1444.
(25) Antony, P. J.; Chongdar, S.; Kumar, P.; Raman, R. *Electrochim. Acta* **2007**, *52*, 3985−3994.
(26) Zhu, X. Y.; Bai, R. B.; Wee, K. H.; Liu, C. K.; Tang, S. L. *J. Membr. Sci.* **2010**, *363*, 278−286.
(27) Zhao, G. J.; Stevens, S. E. *Biometals* **1998**, *11*, 27−32.
(28) Lok, C. N.; Ho, C. M.; Chen, R.; He, Q. Y.; Yu, W. Y.; Sun, H.; Tam, P. K.; Chiu, J. F.; Chen, C. M. *J. Proteome Res.* **2006**, *5*, 916−924.
(29) Bera, S.; Gangopadhyay, P.; Nair, K. G.; Panigrahi, B. K.; Narasimhan, S. V. *J. Electron. Spectrosc.* **2006**, *152*, 91−95.
(30) Scardino, A.; Denys, R.; Ison, O.; O'Connor, W.; Steinberg, P. *Biofouling* **2003**, *19*, 221−230.
(31) Bers, A. V.; Wahl, M. *Biofouling* **2004**, *20*, 43−51.
(32) Callow, M. E.; Jennings, A. R.; Brennan, A. B.; Seegert, C. A.; Wilson, L.; Feinberg, A.; Baney, R.; Callow, J. A. *Biofouling* **2002**, *18*, 237−245.
(33) Berntsson, K. M.; Jonsson, P. R.; Lejhall, M.; Gatenholm, P. *J. Exp. Mar. Biol. Ecol.* **2000**, *251*, 59−83.
(34) Hoipkemeier, W. L.; Schumacher, J. F.; Carman, M. L.; Gibson, A. L.; Feinberg, A. W.; Callow, M. E.; Scheuerman, T. R.; Camper, A. K.; Hamilton, M. A. *J. Colloid Interface Sci.* **1998**, *208*, 23−33.
(35) Dong, B.; Manolache, S.; Somers, E. B.; Wong, A.; Denes, F. S. *J. Appl. Polym. Sci.* **2005**, *97*, 485−497.
(36) Banerjee, I.; Pangule, R. C.; Kane, R. S. *Adv. Mater.* **2011**, *23*, 690−718.
(37) Asharani, P. V.; Mun, L. G.; Hande, M. P.; Valiyaveettil, S. *ACS. Nano* **2009**, *3*, 279−290.